

New  $\mu$ s isomers in the neutron-rich  $^{210}\text{Hg}$  nucleus

A. Gottardo<sup>a,b,\*</sup>, J.J. Valiente-Dobón<sup>a</sup>, G. Benzoni<sup>c</sup>, A. Gadea<sup>d</sup>, S. Lunardi<sup>b,e</sup>, P. Boutachkov<sup>f</sup>, A.M. Bruce<sup>g</sup>, M. Górska<sup>f</sup>, J. Grebosz<sup>h</sup>, S. Pietri<sup>f</sup>, Zs. Podolyák<sup>i</sup>, M. Pfützner<sup>j</sup>, P.H. Regan<sup>i</sup>, H. Weick<sup>f</sup>, J. Alcántara Núñez<sup>k</sup>, A. Algora<sup>d</sup>, N. Al-Dahan<sup>i</sup>, G. de Angelis<sup>a</sup>, Y. Ayyad<sup>k</sup>, N. Alkhomashi<sup>l</sup>, P.R.P. Allegro<sup>m</sup>, D. Bazzacco<sup>e</sup>, J. Benlliure<sup>k</sup>, M. Bowry<sup>i</sup>, A. Bracco<sup>c,n</sup>, M. Bunce<sup>g</sup>, F. Camera<sup>c,n</sup>, E. Casarejos<sup>o</sup>, M.L. Cortes<sup>f</sup>, F.C.L. Crespi<sup>c</sup>, A. Corsi<sup>c,n</sup>, A.M. Denis Bacelar<sup>g</sup>, A.Y. Deo<sup>i</sup>, C. Domingo-Pardo<sup>f</sup>, M. Doncel<sup>p</sup>, Zs. Dombradi<sup>q</sup>, T. Engert<sup>f</sup>, K. Eppinger<sup>r</sup>, G.F. Farrelly<sup>i</sup>, F. Farinon<sup>f</sup>, E. Farnea<sup>e</sup>, H. Geissel<sup>f</sup>, J. Gerl<sup>f</sup>, N. Goel<sup>f</sup>, E. Gregor<sup>f</sup>, T. Habermann<sup>f</sup>, R. Hoischen<sup>f,s</sup>, R. Janik<sup>t</sup>, P.R. John<sup>b,e</sup>, S. Klupp<sup>r</sup>, I. Kojouharov<sup>f</sup>, N. Kurz<sup>f</sup>, S.M. Lenzi<sup>b,e</sup>, S. Leoni<sup>c,n</sup>, S. Mandal<sup>u</sup>, R. Menegazzo<sup>e</sup>, D. Mengoni<sup>e</sup>, B. Million<sup>c</sup>, V. Modamio<sup>a</sup>, A.I. Morales<sup>c</sup>, D.R. Napoli<sup>a</sup>, F. Naqvi<sup>f,v</sup>, R. Nicolini<sup>c,n</sup>, C. Nociforo<sup>f</sup>, A. Prochazka<sup>f</sup>, W. Prokopowicz<sup>f</sup>, F. Recchia<sup>e</sup>, R.V. Ribas<sup>m</sup>, M.W. Reed<sup>i</sup>, D. Rudolph<sup>s</sup>, E. Sahin<sup>a</sup>, H. Schaffner<sup>f</sup>, A. Sharma<sup>f</sup>, B. Sitar<sup>t</sup>, D. Siwal<sup>u</sup>, K. Steiger<sup>r</sup>, P. Strmen<sup>t</sup>, T.P.D. Swan<sup>i</sup>, I. Szarka<sup>t</sup>, C.A. Ur<sup>e</sup>, P.M. Walker<sup>i</sup>, O. Wieland<sup>c</sup>, H.-J. Wollersheim<sup>f</sup>

<sup>a</sup> Istituto Nazionale di Fisica Nucleare, Laboratori Nazionali di Legnaro, Legnaro, 35020, Italy

<sup>b</sup> Dipartimento di Fisica dell'Università degli Studi di Padova, Padova, 35131, Italy

<sup>c</sup> Istituto Nazionale di Fisica Nucleare, Sezione di Milano, Milano, 20133, Italy

<sup>d</sup> Instituto de Física Corpuscular, CSIC-Universitat de València, València, E-46980, Spain

<sup>e</sup> Istituto Nazionale di Fisica Nucleare, Sezione di Padova, Padova, 35131, Italy

<sup>f</sup> GSI Helmholtzzentrum für Schwerionenforschung, Darmstadt, D-64291, Germany

<sup>g</sup> School of Computing, Engineering and Mathematics, University of Brighton, Brighton, BN2 4GJ, United Kingdom

<sup>h</sup> Niewodniczanski Institute of Nuclear Physics, Polish Academy of Science, Krakow, PL-31-342, Poland

<sup>i</sup> Department of Physics, University of Surrey, Guildford, GU2 7XH, United Kingdom

<sup>j</sup> Faculty of Physics, University of Warsaw, Warsaw, PL-00681, Poland

<sup>k</sup> Universidade de Santiago de Compostela, Santiago de Compostela, E-175706, Spain

<sup>l</sup> KACST, Riyadh, 11442, Saudi Arabia

<sup>m</sup> Instituto de Física, Universidade de São Paulo, São Paulo, 05315-970, Brazil

<sup>n</sup> Dipartimento di Fisica dell'Università degli Studi di Milano, Milano, 20133, Italy

<sup>o</sup> EEI, Universidade de Vigo, Vigo, E-36310, Spain

<sup>p</sup> Grupo de Física Nuclear, Universidad de Salamanca, Salamanca, E-37008, Spain

<sup>q</sup> Institute of Nuclear Research of the Hungarian Academy of Sciences, Debrecen, H-4001, Hungary

<sup>r</sup> Physik Department, Technische Universität München, Garching, D-85748, Germany

<sup>s</sup> Department of Physics, Lund University, Lund, S-22100, Sweden

<sup>t</sup> Faculty of Mathematics and Physics, Comenius University, Bratislava, 84215, Slovakia

<sup>u</sup> Department of Physics and Astrophysics, University of Delhi, Delhi, 110007, India

<sup>v</sup> Institut für Kernphysik, Universität zu Köln, Köln, D-50937, Germany

## ARTICLE INFO

## Article history:

Received 12 April 2013

Received in revised form 22 July 2013

Accepted 25 July 2013

Available online 31 July 2013

Editor: V. Metag

## ABSTRACT

Neutron-rich nuclei in the lead region, beyond  $N = 126$ , have been studied at the FRS-RISING setup at GSI, exploiting the fragmentation of a primary uranium beam. Two isomeric states have been identified in  $^{210}\text{Hg}$ : the  $8^+$  isomer expected from the seniority scheme in the  $\nu g_{9/2}$  shell and a second one at low spin and low excitation energy. The decay strength of the  $8^+$  isomer confirms the need of effective three-body forces in the case of neutron-rich lead isotopes. The other unexpected low-lying

\* Corresponding author at: Istituto Nazionale di Fisica Nucleare, Laboratori Nazionali di Legnaro, Legnaro, 35020, Italy.  
E-mail address: [andrea.gottardo@lnl.infn.it](mailto:andrea.gottardo@lnl.infn.it) (A. Gottardo).

isomer has been tentatively assigned as a  $3^-$  state, although this is in contrast with theoretical expectations.

© 2013 Elsevier B.V. All rights reserved.

Atomic nuclei are complex many-body systems with many degrees of freedom; nevertheless their spectral properties often show very regular features due to the symmetries of the nuclear Hamiltonian. A remarkable example of this is offered by the occurrence of the seniority excitation scheme in spherical, semi-magic nuclei [1]. A deviation from this regular behaviour suggests a change in the underlying nuclear structure, as for example a sudden onset of deformation. The neutron-rich regions around double shell closures have been studied for light and medium-mass nuclei, using fission and deep-inelastic reactions. However, the neutron-rich region around  $^{208}\text{Pb}$  has not been thoroughly explored so far, due to its high mass and neutron richness. Pioneering work has been reported in Refs. [2,3]. A deeper knowledge would be desirable, since  $^{208}\text{Pb}$  is a benchmark for the study of nuclear structure thanks to its double-shell closure character. For semi-magic neutron-rich  $^{210-216}\text{Pb}$  isotopes, a standard seniority structure has been found, as it is expected from neutrons in the  $2g_{9/2}$  shell [4]. A  $8^+$  isomer was measured in each isotope (with  $t_{1/2}$  in the range  $\sim 0.1-6 \mu\text{s}$ ), decaying via the  $6^+ \rightarrow 4^+ \rightarrow 2^+ \rightarrow 0^+$  yrast cascade, with the levels spaced with decreasing energies as the spin increases. The analysis of the transition rates from the isomeric states allowed one to assess the role played by the usually neglected effective three-body forces, arising from core excitations outside the valence space [4]. Generally, the seniority scheme provided by the coupling of the valence neutrons in the  $g_{9/2}$  shell may also hold when few protons are added to the  $^{208}\text{Pb}$  core. In fact, they can act as spectators, while the angular momentum of the excited states is given by the coupling of the neutrons. This is indeed the case if two protons are added to the  $Z = 82$  core: the resulting polonium isotopes show a  $g_{9/2}$  seniority scheme [5–7], apart from  $^{214}\text{Po}$  whose known level scheme is limited to low-spin states.

Similarly, when two protons are removed from the  $Z = 82$  core, leading to mercury isotopes, one would expect to observe the same  $g_{9/2}$  seniority scheme. The isotope  $^{208}\text{Hg}$  has indeed a  $8^+$  isomer attributed to the maximally-aligned configuration  $\nu g_{9/2}^2$  [8]. In this nucleus, the two proton holes are in the  $s_{1/2}$  and  $d_{3/2}$  orbits, the less bound ones below  $Z = 82$ . They appear to be inactive spectators with respect to the neutron valence space. A similar behaviour is, in principle, expected also in the more neutron-rich isotope  $^{210}\text{Hg}$ , whose level structure was completely unknown up to now.

This Letter reports the first experimental study of excited states in  $^{210}\text{Hg}$  providing evidence of two isomers in the  $\mu\text{s}$  range. One is interpreted as the  $8^+$  isomer expected from the  $g_{9/2}$  seniority scheme, while the other one, for which we tentatively suggest a  $3^-$  assignment, is located at an unexpected low energy, remaining therefore a challenge for future experiments and theoretical models.

Experimentally, nuclei around the  $^{208}\text{Pb}$  region, more than two or three neutrons from stability, have been produced with relatively cold fragmentation reactions from a primary  $^{238}\text{U}$  beam. The results on  $^{210}\text{Hg}$  have been obtained by exploiting the uniqueness of the FRS-RISING setup [9–12] and the UNILAC-SIS accelerator facilities at GSI by using a 1 GeV  $^{238}\text{U}$  beam at an intensity of around  $1.5 \times 10^9$  ions/spill. The  $\sim 1$  s spills were separated by  $\sim 2$  s without beam. The beam impinged on a  $2.5 \text{ g/cm}^2$  Be target followed by a  $223 \text{ mg/cm}^2$  Nb stripper. The isotopes resulting from the fragmentation reaction were separated and identified with the double-stage magnetic spectrometer FRS [9]. The FRS allows one to discriminate the magnetic rigidities of the fragments

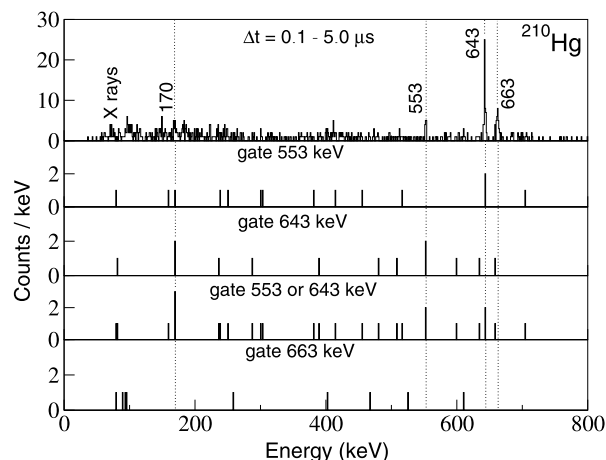


Fig. 1. The upper panel shows the  $\gamma$  spectrum, time-gated ( $\Delta t = 0.1-5.0 \mu\text{s}$ ) for the  $^{210}\text{Hg}$  isotope. The spectra below show the  $\gamma\gamma$  coincidences for the different  $\gamma$  rays.

with a resolution sufficient to distinguish adjacent isotopes even at the high masses of interest ( $A \sim 210-220$ ). The identification in mass over charge ratio ( $A/q$ ) is achieved through time of flight and focal-plane position measurements, while the atomic number is obtained from two ionization chambers placed in the final focal plane. These measurements are sufficient to provide a complete identification of the isotopes event by event. At the final focal plane, the ions were slowed down in a thick Al degrader in order to reduce the energy of the fragments of interest so they could be implanted in a composite double-sided silicon-strip (DSSSD) detector system [12,13]. The DSSSD detector system was surrounded by the RISING  $\gamma$  spectrometer [10,11], with a full-energy  $\gamma$ -ray peak detection efficiency of 15% at 662 keV [10]. Further experimental details can be found in Refs. [4,14].

Fig. 1, upper panel, shows the  $\gamma$ -ray spectrum following the isomeric decays of  $^{210}\text{Hg}$ . After an implantation event, a delayed gate of  $5 \mu\text{s}$  length was used to detect isomers. In total, 936 ions were identified as  $^{210}\text{Hg}$ . Three  $\gamma$  lines are clearly visible at 663, 643 and 553 keV. A fourth line is also identified at 170 keV. The spectra obtained from the  $\gamma\gamma$  coincidence data are also presented in Fig. 1. The background in these highly-selective spectra is almost non-existent and, when two  $\gamma$ -transitions are not in coincidence (see for example the bottom spectrum in Fig. 1), the few counts are distributed randomly in the entire energy range, never exceeding one count per channel. If two lines are in coincidence, as it is the case for those at 553 and 643 keV, this is proven clearly by the concentration of even a small amount of counts at the expected channels (see second and third spectra of Fig. 1). By summing the spectra in coincidence with the 643- and 553-keV lines, the transition at 170 keV is also evident, thereby strengthening its identification as the third member of a  $\gamma$ -ray cascade composed by the 170-, 553- and 643-keV transitions. As stated above, no  $\gamma$  rays are observed in coincidence with the 663-keV line, despite its higher intensity with respect to the 170- and 553-keV transitions. The statistical significance of the absence of coincidences between the 663- and the 643-keV  $\gamma$  rays can be estimated with a binomial distribution, the use of a Poisson distribution being less justified due to the low statistics. The calculation is performed considering

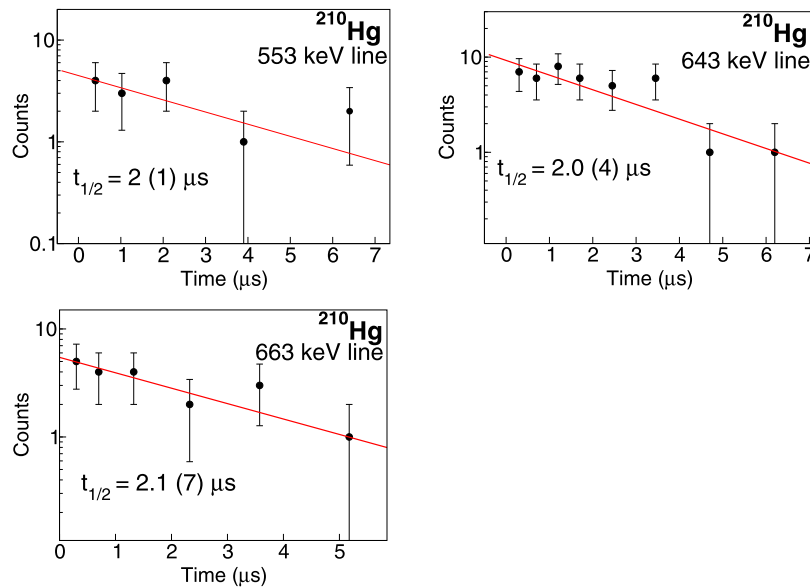


Fig. 2. (Colour online.) Time distributions and the exponential fit in red for the 553-, 643- and 663-keV transitions assigned to  $^{210}\text{Hg}$ .

Table 1

Area, transition intensities corrected for efficiency and internal conversion and their half-life  $t_{1/2}$  for  $^{210}\text{Hg}$ . The line at 170 keV, with its low statistics, is in a too high background region to fit its time distribution.

$E_\gamma$ (keV)	Area	Intensity (%)	$t_{1/2}$ ( $\mu\text{s}$ )
170	13 (7)	22 (12)	–
553	12 (4)	23 (8)	2 (1)
643	45 (7)	100 (16)	2.0 (4)
663	25 (6)	65 (13)	2.1 (7)

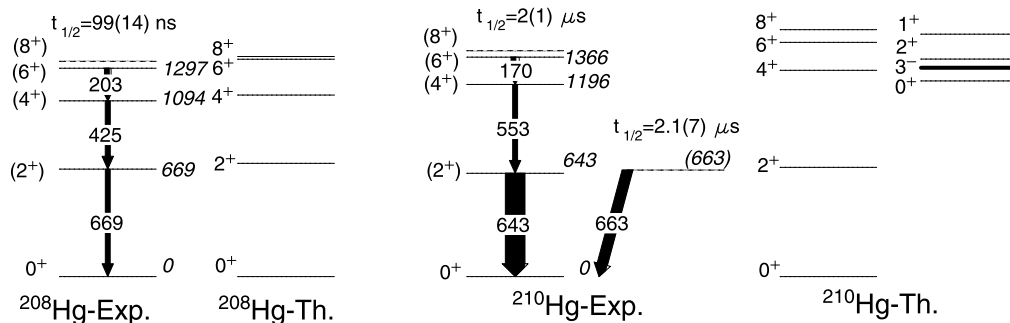
the absolute  $\gamma$  efficiency at 663 keV, estimated to be 12.7%, and the missing feeding of the 643-keV state, which results to be 33 (8) counts. As a consequence, if the 663-keV  $\gamma$  ray feeds with such intensity the  $2^+$  state, the probability of not observing any coincidence between the 643-keV and 663-keV transitions in cascade is only  $1.1^{+2.3}_{-0.7}\%$ . Therefore, the absence of coincidence between the 643- and the 663-keV  $\gamma$  rays is a clear indication that the large intensity of the 643-keV line cannot be attributed to the feeding from the 663-keV  $\gamma$  ray.

Fig. 2 shows the time distributions of the three most intense  $\gamma$  transitions assigned to  $^{210}\text{Hg}$  together with the results of an exponential fit of the data. Within errors, the half lives of the 553- and 643-keV transitions are equal and, being in mutual coincidence, they are assigned to follow the decay of the same isomer. The 663-keV transition shows also a similar half life, but it is not in coincidence with the other  $\gamma$ -rays. Because of intensity reasons (see below), we will conclude that it belongs to the decay of another, low-lying isomer with a half-life similar to the one de-excited by the 170-, 553- and 643-keV sequence.

Table 1 summarizes the intensities of the  $\gamma$  rays assigned to  $^{210}\text{Hg}$  and the half-lives derived from their time distributions. The 170- and 553-keV lines have comparable intensities, while the 643- and 663-keV  $\gamma$  rays have much larger intensity. The combination of this experimental information with the expected systematics of neutron-rich even-even Hg nuclei [8] allows one to assign the three transitions in mutual coincidence of 170, 553, and 643 keV to the de-excitation of the  $8^+$  isomer, similarly to what is observed in  $^{208}\text{Hg}$  [8] or in the even-even Pb isotopes [4]. The three  $\gamma$  rays are then attributed to the  $6^+ \rightarrow 4^+ \rightarrow 2^+ \rightarrow 0^+$  decay sequence. The  $8^+ \rightarrow 6^+$  is not detected because of its low energy and, as discussed in Refs. [4,8], it is assumed to be between

20 and 80 keV. In fact, the characteristic  $K_\alpha$  X rays from mercury at 71 keV are compatible with their origin from the 170-keV transition only: therefore, it is inferred that the  $8^+ \rightarrow 6^+$  energy must be below the 78 keV binding energy of the mercury K electrons, hence the given upper limit. From systematics, a conservative lower limit of 20 keV is adopted.

Fig. 3 shows the level scheme deduced for  $^{210}\text{Hg}$  compared with the one of  $^{208}\text{Hg}$  [8]. The sequence  $6^+ \rightarrow 4^+ \rightarrow 2^+ \rightarrow 0^+$  from the decay of the  $8^+$  isomer follows closely the systematics of the  $g_{9/2}$  seniority isomers and it is in good agreement, within 100 keV, with state-of-the-art shell-model calculations, shown in the same figure. Theoretical calculations were performed using the shell-model codes ANTOINE and NATHAN [15,16], and the Kuo–Herling interaction (KH) [17], slightly modified as indicated in Ref. [8]. The experimental spectrum of  $^{209}\text{Pb}$  was used for the single-particle energies. The neutron valence space considered was  $(g_{9/2}i_{11/2}j_{15/2})^4$  above the closed  $N = 126$  core and the proton valence space was  $(2d_{5/2}2d_{3/2}h_{11/2}s_{1/2})^{-2}$  below the  $Z = 82$  shell closure (it is a two proton-hole space). Assuming that the decay curve of the  $4^+ \rightarrow 2^+$  transition is due to the lifetime of the feeding  $8^+$  isomer, and with the aforementioned energy limits on this level, the  $B(E2)$  from the isomeric state ranges from 5 (2) to 6 (2)  $e^2 \text{ fm}^4$ . The value predicted by shell model calculations is  $55 e^2 \text{ fm}^4$ , using the effective charges  $e_\nu = 1.0e$  and  $e_\pi = 1.5e$  as in the case of  $^{208}\text{Hg}$  [8], where the agreement with the measured value was very good. In  $^{210}\text{Hg}$ , on the contrary, the shell-model calculation overestimates the  $B(E2)$  by a factor nine, similarly to what observed in the analogous four-valence-neutrons  $^{212}\text{Pb}$  [4]. This would require the use of effective charges for neutrons and protons much lower than the standard ones. The state dependence of the effective charges is most probably related to the neglect of  $0\hbar\omega$  excitations across the  $^{208}\text{Pb}$  core and of the associated effective three-body components of the nuclear Hamiltonian, as it has been discussed extensively in Ref. [4]. In that publication it was shown how the particle-hole excitations, coming from the lead core, play a major role in determining the values of the effective charge and how this contribution cannot be renormalized via the use of a constant effective charge. Actually, the same mechanism is expected to take place in  $^{210}\text{Hg}$ , because the neutrons and protons occupy the same  $\Delta\hbar\omega = 0$  relevant orbitals ( $\nu 0i_{13/2} - \nu 1g_{9/2}$  and  $\pi 0h_{11/2} - \pi 1f_{7/2}$ ) as  $^{212}\text{Pb}$ . The proton-hole wave function is



**Fig. 3.** Experimental and calculated level schemes of  $^{208,210}\text{Hg}$ . The 663-keV state in  $^{210}\text{Hg}$  is tentatively identified. The  $3^-$  state in  $^{210}\text{Hg}$ , calculated via particle-vibration models, is thicker to distinguish it from the other levels calculated with the shell-model. The experimental data for  $^{208}\text{Hg}$  are taken from Ref. [8].

mainly in the  $\pi d_{3/2}$  and  $\pi s_{1/2}$  orbitals below  $Z = 82$ : this implies a very weak contribution to the  $\Delta J = 2$  particle-hole jumps responsible for quadrupole coherence [4]. Exact calculations are not possible at the moment but the two proton holes are not expected to play a role in the structure of the seniority isomer. The isomer should thus have the same structure of the one of neutron-rich lead isotopes. The overestimation of the  $B(E2)$  in  $^{210}\text{Hg}$  of roughly the same amount as in the isotone  $^{212}\text{Pb}$  appears as a confirmation of the importance of effective three-body forces in this region.

Besides the seniority-scheme isomer, it is evident from the upper panel of Fig. 1 that the intensity of the  $2^+ \rightarrow 0^+$  transition is four times larger than the intensity of the  $\gamma$  ray (553 keV) directly feeding the  $2^+$ . This requires the presence of another isomeric state whose decay feeds, for three quarters of its population, the  $2^+$  state. This must be due to the other isomer that, as seen experimentally, exists in  $^{210}\text{Hg}$ . A single transition that could explain the intensity missing in the  $2^+$  level should have three times the intensity of the 553-keV  $\gamma$  ray. Therefore, it should be clearly visible in the data, unless it is of low energy where internal conversion becomes dominant. No further transitions, besides the 170- and the 553-keV ones, are however observed in coincidence with the 643-keV line, pointing to a non-measurable transition connecting the other isomer to the  $2^+$  state. If an observational limit of five counts is set, this transition must be below 40 keV, 150 keV, 200 keV and 260 keV for E1, E2, M1, and E3 multiplicities, respectively. The fact that the quite intense delayed transition at 663 keV is not in coincidence with any other line could suggest that it connects directly the other isomer to the  $0^+$  ground state. This scenario, illustrated in Fig. 3, is also compatible with a direct decay of the new isomer to the  $2^+$  state through a strongly converted 20-keV transition, as required by the high intensity of the  $2^+ \rightarrow 0^+$  transition. The proposed state at 663 keV, because of its decay to both the  $0^+$  ground state and to the  $2^+$  state, can assume only spins from 1 to 3. The low spin of this isomer is also supported by the analysis of the isomeric ratio, performed using the method described in Ref. [18].

The isomeric ratio is, for each isotope and each isomer, the ratio between the number of nuclei populated in their excited isomeric state and the total number of ions of that nuclide produced after a fragmentation reaction. The final value takes into account the loss of ions in excited states due to the time of flight in the FRS and the loss in RISING  $\gamma$  efficiency due to the prompt  $\gamma$  flash [18]. In the scenario proposed in Fig. 3 for  $^{210}\text{Hg}$ , the values obtained are 0.11 (4) for the  $8^+$  isomer and 0.6 (1) for the isomer at 663 keV, supposing it feeds the  $2^+$  state. If only the yield of the 663 keV-line is used, then the isomeric ratio of this level would be 0.25 (6). Therefore, in any case the relative population of the two isomers is suggesting that the spin of the 663-keV state is quite low, in particular lower than  $8^+$ , and that it is an yrast state [19]. In fact, the

**Table 2**

Experimental reduced transition strengths  $B(E, M\lambda)$  in Weisskopf units. The branching ratio is 0.43 (9) and 0.57 (9) for the 663- and 20-keV transitions, respectively.

$E_\gamma$ (keV)	$E, M\lambda$	$B(E, M\lambda)$ (W.u.)
663	E1	$3 (1) \cdot 10^{-10}$
663	E2	$3 (1) \cdot 10^{-5}$
663	E3	4 (2)
663	M1	$4 (1) \cdot 10^{-8}$
20	M1	$8 (3) \cdot 10^{-6}$
20	E1	$1.5 (6) \cdot 10^{-6}$

schematic sharp cutoff model [18] predicts an increasing population with decreasing spin.

The lifetime derived from the decay curve of the 663-keV line (see Fig. 1) will help to discriminate among the possible spin-parities of the proposed low-spin isomer by deducing the transition probabilities for the different possible multiplicities involved. Table 2 shows the Weisskopf strengths of the various multiplicities for the proposed 20- and 663-keV transitions. The resulting transition rates appear in most cases very much hindered, at variance with systematics, with the exception of the E3 case for the 663-keV energy and the E1 case for the 20-keV energy. In fact, E3 transitions are normally of the order of one to several W.u., while a suppression factor of  $10^6$  for E1 transitions is not uncommon [20]. Therefore, a  $3^-$  assignment for the 663-keV state seems the most reasonable based on the reduced transition probabilities. This in fact would give a 663-keV E3 transition to the ground state and a 20-keV E1 transition to the  $2^+$  level.

Other possibilities are discussed in the following. A  $1^+$  assignment would give a 663-keV M1 transition hindered by a factor  $10^8$ , which is not realistic, even for an  $\ell$ -forbidden M1. For example, in the one-proton hole  $^{207}\text{Tl}$  isotope, there is a  $3/2^+$  state (configuration  $(\pi d_{3/2})^{-1}$ ) decaying to the ground state  $1/2^+$  (configuration  $(\pi s_{1/2})^{-1}$ ), with a half life of 30 ps. This is a  $\ell$ -forbidden M1 transition, of  $\sim 10^{-2}$  W.u.,  $10^6$  times higher than in the present case. A  $2^+$  assignment would give an E2 transition suppressed by a factor  $10^5$ , which is against all the systematics in literature. Finally, the large hindrance,  $10^{-10}$  required to justify an isomeric  $1^-$  663-keV state rules out also this possibility.

For the level scheme proposed for  $^{210}\text{Hg}$  in Fig. 3, the analysis of the transition probabilities favours therefore a  $3^-$  spin-parity assignment to the state at 663 keV. All the other scenarios are incompatible with the measured lifetimes and intensities. In summary, the experimental data, i.e.  $\gamma\gamma$  coincidences, half-life and branching ratio, suggest a possible level scheme as the one shown in Fig. 3, where the 663-keV state has most probably a  $3^-$  character.

In the following, theoretical predictions for the 663-keV transition in  $^{210}\text{Hg}$  will be discussed, pointing out the difficulty to

explain the lower energy isomer. The shell model calculations, discussed previously and successful in reproducing the sequence of states populated by the  $8^+$  isomer and the isomer lifetime (once the problem of neglecting effective three-body forces is considered), predict the second  $0^+$  at 1.1 MeV, the  $1^+$  state at 1.5 MeV, the  $1^-$  level at 2.7 MeV and the second  $2^+$  at 1.34 MeV (see Fig. 3), but cannot reliably predict the location of a  $3^-$  state. This is because the present shell-model calculations do not allow core excitations and it is known that the  $3^-$  state in the lead region is very fragmented [21], involving many particle-hole excitations across the  $^{208}\text{Pb}$  core. As a consequence, shell model calculations do not predict any excited state below 1.1 MeV, apart from the first excited  $2^+$  state. By looking at the systematics of  $3^-$  excitations in this region, one observes that the  $3^-$  level is at 2.6 MeV in  $^{208}\text{Pb}$  and drops to 1.9 MeV in  $^{210}\text{Pb}$  due to mixing between the collective  $^{208}\text{Pb}$  octupole phonon and the  $3^-$  originating from the octupole coupling of the  $\Delta J = \Delta \ell = 3$  neutron shells  $g_{9/2} - j_{15/2}$  [21]. In more neutron-rich nuclei, further reduction of the excitation energy is expected [21]. For example, in  $^{214}\text{Po}$ , which has the same neutron number of  $^{210}\text{Hg}$  and two protons above  $Z = 82$  ( $^{210}\text{Hg}$  has two protons below), the energy of the  $3^-$  state is at around 1.3 MeV [22], the value which is predicted also in  $^{210}\text{Hg}$  by particle-vibration coupling models [21], as shown in Fig. 3. These calculations are very reliable, since they reproduce quite accurately the energy of the  $3^-$  states in the region. A  $3^-$  state at only 663 keV is therefore in contrast with basic theoretical expectations.

In conclusion, the very exotic  $^{210}\text{Hg}$  nucleus was investigated for the first time via isomer decay spectroscopy. Its production and study were made possible thanks to state-of-the-art improvements in experimental techniques and to the intense uranium beams provided by the accelerator complex at GSI. A sequence of positive parity states  $0^+$ ,  $2^+$ ,  $4^+$ ,  $6^+$  is proposed to belong to the decay of the  $8^+$  seniority isomer. This sequence, very similar to that of the neighbouring  $^{208}\text{Hg}$ , is well reproduced by shell-model calculations. The decay strength of the isomer is not well reproduced by shell-model calculations, confirming the important role played by effective three-body forces in this region [4]. The experimental data indicate also the presence of another isomer at 663 keV. From its lifetime it was tentatively assigned as a  $J^\pi = 3^-$  state, which is not theoretically expected at such low energy by particle-vibration coupling models. In fact, in almost spherical nuclei, not

too far from the doubly-magic  $^{208}\text{Pb}$ ,  $3^-$  excitations are predicted at higher energy. Such a large drop of the  $3^-$  excitation in  $^{210}\text{Hg}$ , if proven by more sophisticated and high statistics experiments, will be a real challenge for present theoretical models: *ad augusta per angusta*. An important future experimental development will be to directly measure the mass of the isomeric state feeding the  $2^+$  state with storage rings [23].

## Acknowledgements

We are grateful to I. Hamamoto for enlightening discussions on the possible spin-parities of the 663-keV state. The excellent work of GSI accelerator staff is acknowledged. A.G., M.D. and E.F. acknowledge the support of INFN, Italy and MICINN, Spain, through the AIC10-D-000568 bilateral action. A.G. activity has been partially supported by MICINN, Spain and the Generalitat Valenciana, Spain, under grants FPA2008-06419 and PROMETEO/2010/101. The support of the UK STFC, the Swedish Science Council and of the DFG (EXC 153) is also acknowledged.

## References

- [1] A. de Sahlit, I. Talmi, *Nuclear Shell Theory*, Dover Publications, 1963.
- [2] M. Pfützner, et al., *Phys. Lett. B* 444 (1998) 32.
- [3] S.J. Steer, et al., *Phys. Rev. C* 78 (2008) 061302(R).
- [4] A. Gottardo, et al., *Phys. Rev. Lett.* 109 (2012) 162502.
- [5] A. Poletti, et al., *Nucl. Phys. A* 473 (1987) 595.
- [6] J. Kurpeta, et al., *Eur. Phys. J. A* 7 (2000) 49.
- [7] H. De-Witte, et al., *Phys. Rev. C* 69 (2004) 044305.
- [8] N. Al-Dahan, et al., *Phys. Rev. C* 80 (2009) 061302(R).
- [9] H. Geissel, et al., *Nucl. Instr. Meth. B* 70 (1992) 286.
- [10] S. Pietri, et al., *Nucl. Instr. Meth. B* 261 (2007) 1079.
- [11] P.H. Regan, et al., *Nucl. Phys. A* 787 (2007) 491c.
- [12] R. Kumar, et al., *Nucl. Instr. Meth. A* 598 (2009) 754.
- [13] P.H. Regan, et al., *Int. J. Mod. Phys. E* 17 (2008) 8.
- [14] G. Benzoni, et al., *Phys. Lett. B* 715 (2012) 293.
- [15] E. Caurier, F. Nowacki, *Acta Phys. Pol. B* 30 (1999) 705.
- [16] E. Caurier, et al., *Phys. Rev. C* 59 (1999) 2033.
- [17] E.K. Warburton, B.A. Brown, *Phys. Rev. C* 43 (1991) 602.
- [18] M. Pfützner, et al., *Phys. Rev. C* 65 (2002) 064604.
- [19] S.J. Steer, et al., *Phys. Rev. C* 84 (2008) e044313.
- [20] C.H. Perdrisat, *Rev. Mod. Phys.* 38 (1966) 41.
- [21] I. Hamamoto, *Phys. Rep.* 10 (1974) 63.
- [22] S.C. Wu, et al., *Nuclear Data Sheets* 110 (2009) 681.
- [23] M. Reed, et al., *Phys. Rev. Lett.* 105 (2010) 172501.